Modern Numerical Methods with Medical Applications
EEG/MEG based Source Location in the Human Brain

Wolfgang Hackbusch

Max-Planck-Institut für *Mathematik in den Naturwissenschaften*

Inselstr. 22-26, 04103 Leipzig, Germany
wh@mis.mpg.de

http://www.mis.mpg.de/scicomp/hackbusch_e.html

Havanna, 2023

1 Medical background: Epilepsy

An epileptic seizure (convulsión) is the clinical manifestation of an abnormal, excessive, purposeless and synchronized electrical discharge in the brain cells called neurons [Wikipedia]

EEG (Electroencephalography) images the spontaneous electrical activity of the brain.

.

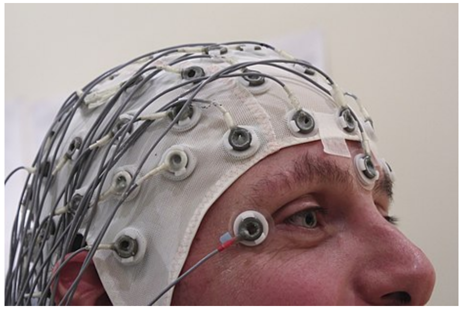

Cap with EEG sensors [Wikipedia]

MEG (Magnetoencephalography) maps the brain activity by recording magnetic fields produced by electrical currents in the brain.

For a presurgical epilepsy diagnosis it is important to detect the location of the source sufficiently accurate (by non-invasing methods).

To be done:

⧫ Imaging of the brain of the individual patient (no general model).

⧫ Creating a Finite Element Mesh of the brain.

⧫ EEG and MEG measurements of the epileptic activity.

⧫ The EEG and MEG data measures the fields at the location of the electrodes. The source reconstruction is an inverse problem. In general, such inverse problems are ill-posed. However, here the situation is simpler since the source is concentrated at one neuron, i.e., the mathematical source term is a delta function.

⧫ All this must be done in a short time.

Details

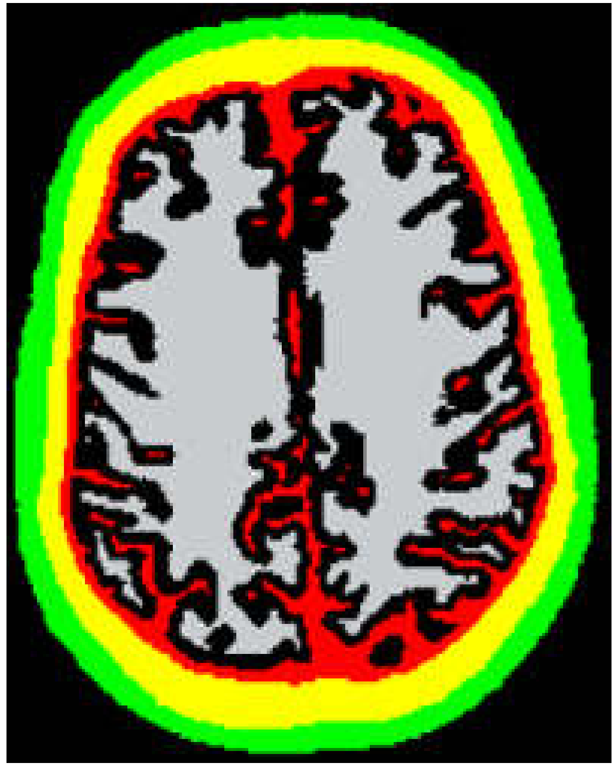

The brain (see cross section) consists of

- scalp - Cuero cabelludo - in green
- skull (bone) - Cráneo - in yellow
- CSF (cerebrospinal fluid) - Líquido cefalorraquídeo - in red
- gray matter - Sustancia gris - contains the neurons - in black
- white matter - Sustancia blanca - in white

2 The Physics Behind

2.1 Maxwell's Equations

The electric and magnetic fields are described by Maxwell's equations. Here, the magnetic permeability μ is constant and equal to the permeability of vacuum.

The primary current during an epileptic seizure can be described by a mathematical dipole at position $\mathbf{x}_0 \in \mathbb{R}^3$ with the moment $\mathbf{M} \in \mathbb{R}^3$:

$$\mathbf{j}(\mathbf{x}) := \mathbf{M}\delta(\mathbf{x} - \mathbf{x}_0).$$

The electric field is

$$\mathbf{E} = -\operatorname{grad} u,$$

where the electric potential u is the solution of the Poisson-like equation

$$\operatorname{div}(\boldsymbol{\sigma} \operatorname{grad} u) = \operatorname{div} \mathbf{j} =: J.$$

Here, $\boldsymbol{\sigma} \in \mathbb{R}^{3\times 3}$ is the so-called *conductivity tensor*.

The equation $\operatorname{div}(\boldsymbol{\sigma} \operatorname{grad} u) = J^P$ is be understood in the weak form.
At interior boundaries γ, where $\boldsymbol{\sigma}$ has a jump discontinuity,

$$\langle \boldsymbol{\sigma}_1 \operatorname{grad} u_1, \mathbf{n} \rangle |_\gamma = \langle \boldsymbol{\sigma}_2 \operatorname{grad} u_2, \mathbf{n} \rangle |_\gamma$$

holds ($\mathbf{n}$: normal direction, $\boldsymbol{\sigma}_1$, u_1 limit values from the left, $\boldsymbol{\sigma}_2$, u_2 limit values from the right).

Finally, we have the *boundary condition*

$$\langle \boldsymbol{\sigma} \operatorname{grad} u, \mathbf{n} \rangle |_\Gamma = 0.$$

Since u is determined up to a constant, we may set

$$u_{\mathrm{ref}} = 0$$

for one reference electrode.

2.2 Magnetic Field

The magnetic field is measured by a magnetometer as in the picture. Let Υ be the path corresponding to the lower part of the magnetometer and set

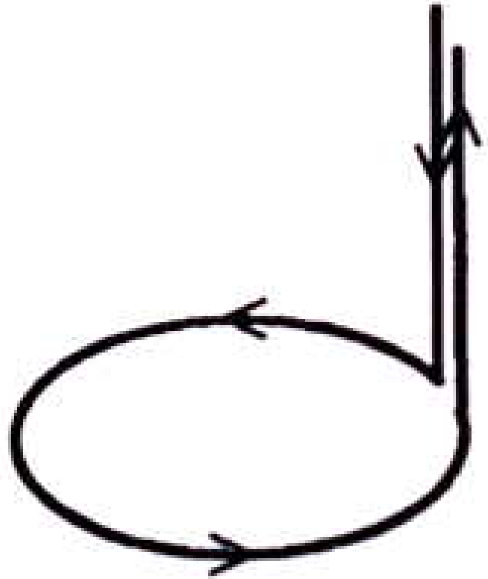

$$\mathbf{C}(\mathbf{y}) := \int_{\Upsilon} \frac{\mathrm{d}\mathbf{x}}{|\mathbf{x} - \mathbf{y}|} \in \mathbb{R}^3,$$

$$\Psi_p := \frac{\mu}{4\pi} \langle \mathbf{M}, \mathbf{C}(\mathbf{x}_0) \rangle, \quad \mu \text{ permeability},$$

$$\Psi_s := -\frac{\mu}{4\pi} \int_{\Omega} \langle \boldsymbol{\sigma}(\mathbf{y}) \operatorname{grad} u(\mathbf{y}), \mathbf{C}(\mathbf{y}) \rangle \, \mathrm{d}\mathbf{y}.$$

Then $\Psi := \Psi_p + \Psi_s$ is the magnetic flux through Υ.

2.3 Forward Problem - Inverse Problem

Forward Problem:

For a fixed source point $\mathbf{x}_0$ solve the PDE for u. Then an epileptic seizure at $\mathbf{x}_0$ would yield EEG values

$$e_i(\mathbf{x}_0) \qquad (i \in I_{\text{EEG}})$$

for the electric field $E = -\,\text{grad}\ u$ at sensor i. Similarly, MEG would yield

$$m_i(\mathbf{x}_0) \qquad (i \in I_{\text{MEG}}).$$

The idea for solving the inverse problem is:
Given the tuples $\left\{(e_i)_{i \in I_{EEG}}\right\}$ and $\left\{(m_i)_{i \in I_{MEG}}\right\}$ for many source points $\mathbf{x}_0$, search for $\mathbf{x}_0$ with the best fit to the measured data (e_i, m_i).

3 FEM Approach

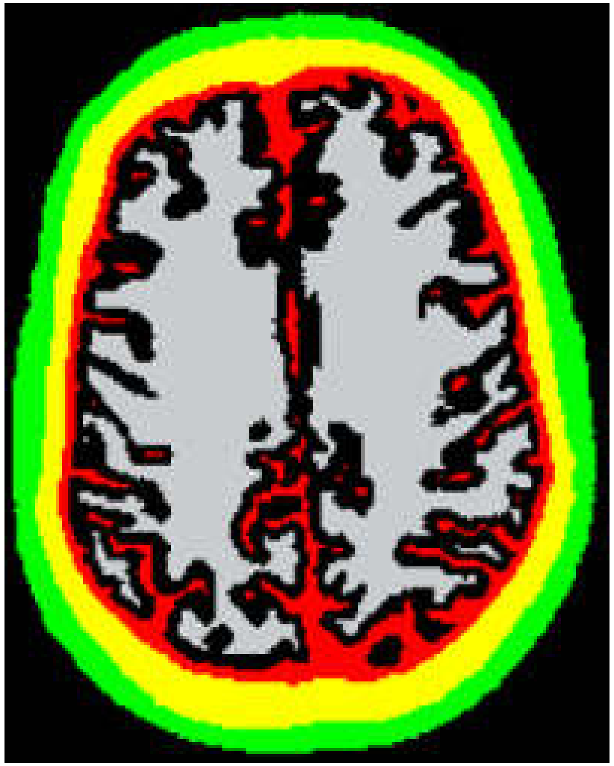

Repeated:

3.1 Mesh Generation

Simplest approach: direct use of the voxels of the MRI* images by cubes, possibly after coarsening.

This is insufficient because of the interior boundaries. *Remedy:* node shift (see picture)

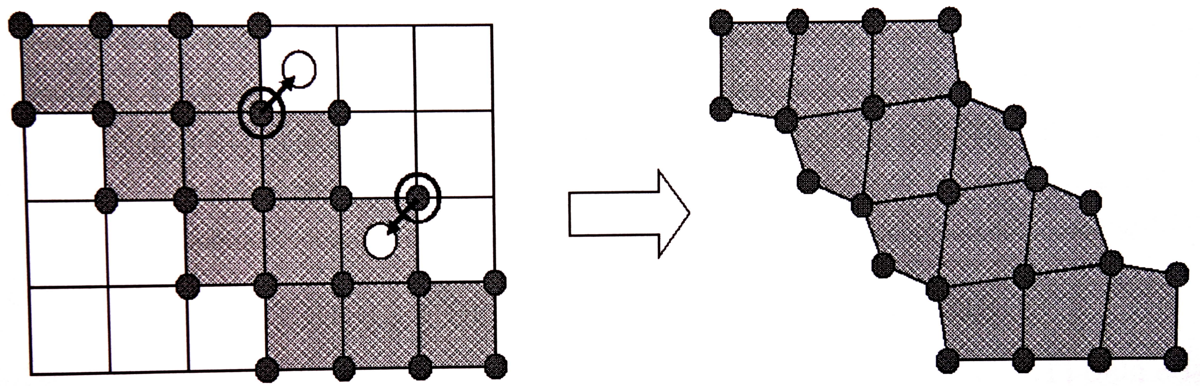

Most flexible approach: tetrahedra, again alined to interior boundaries.

*MRI = Magnetic Resonance Imaging

More general FE approaches:

- Mixed finite elements

  Vorwerk, J., Engwer, C., Pursiainen, S. and Wolters, C.H., *A Mixed Finite Element Method to Solve the EEG Forward Problem*, IEEE Transactions on Medical Imaging, 36(4):930-941 (2017).

- Discontinuous finite elements

  Engwer, C., Vorwerk, J., Ludewig, J. and Wolters, C.H., *A Discontinuous Galerkin Method for the EEG Forward Problem*, SIAM J. on Scientific Computing, 39 (1), B138–B164 (2017)

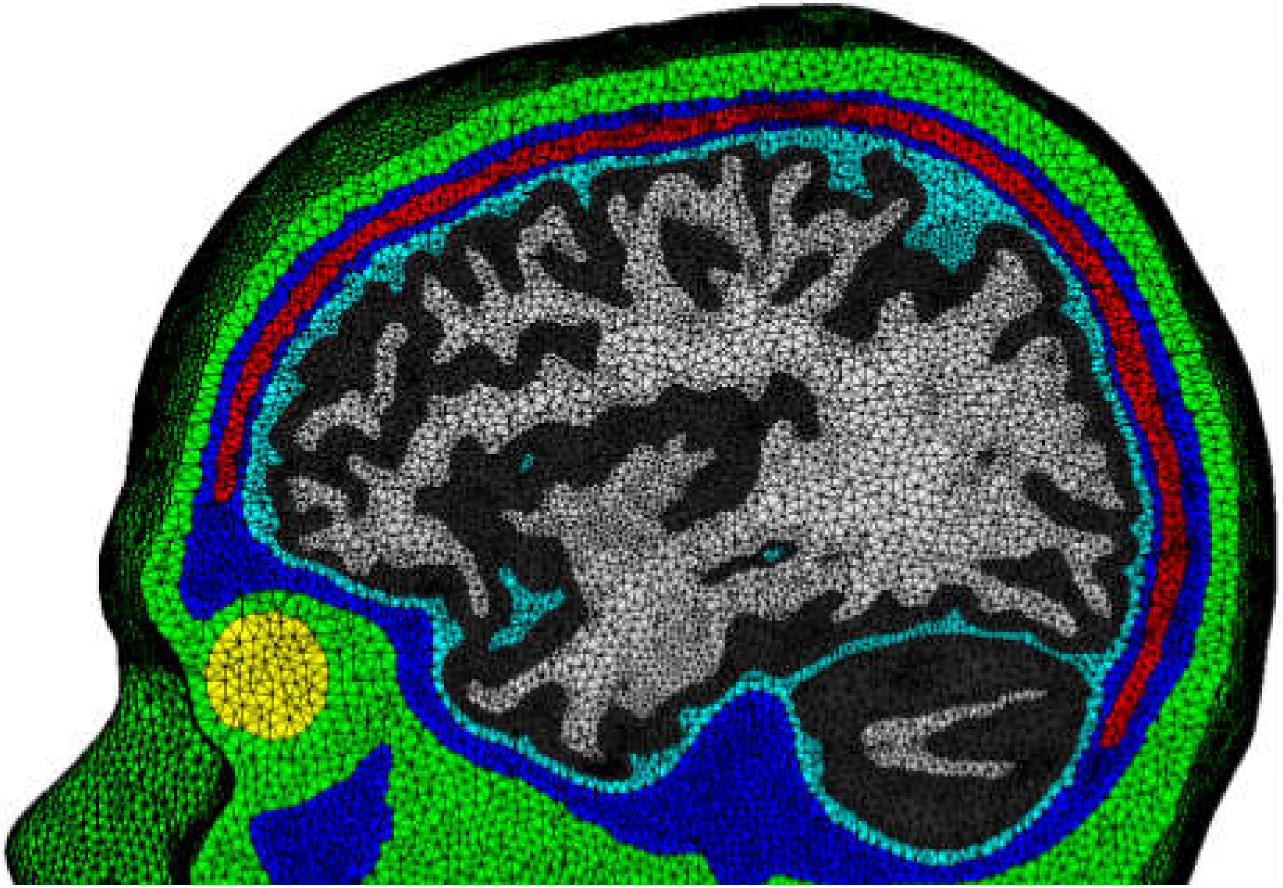

Example of a FE triangulation (cross section)

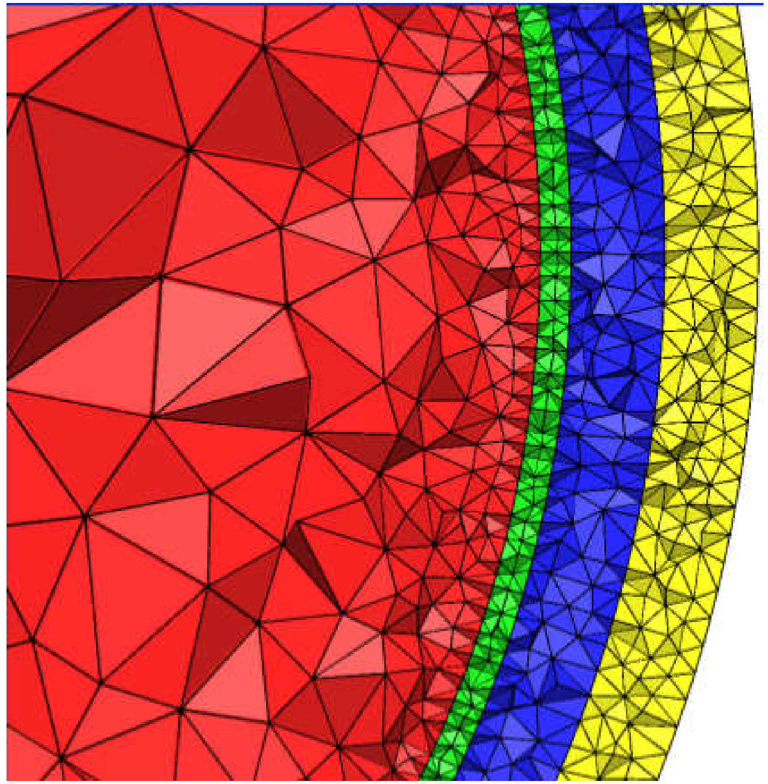

Local refinement / coarsening

The modelling needs special care in defining the **electric conductivity**, which is anisotropic for the scull and white matter (direction of fibers).

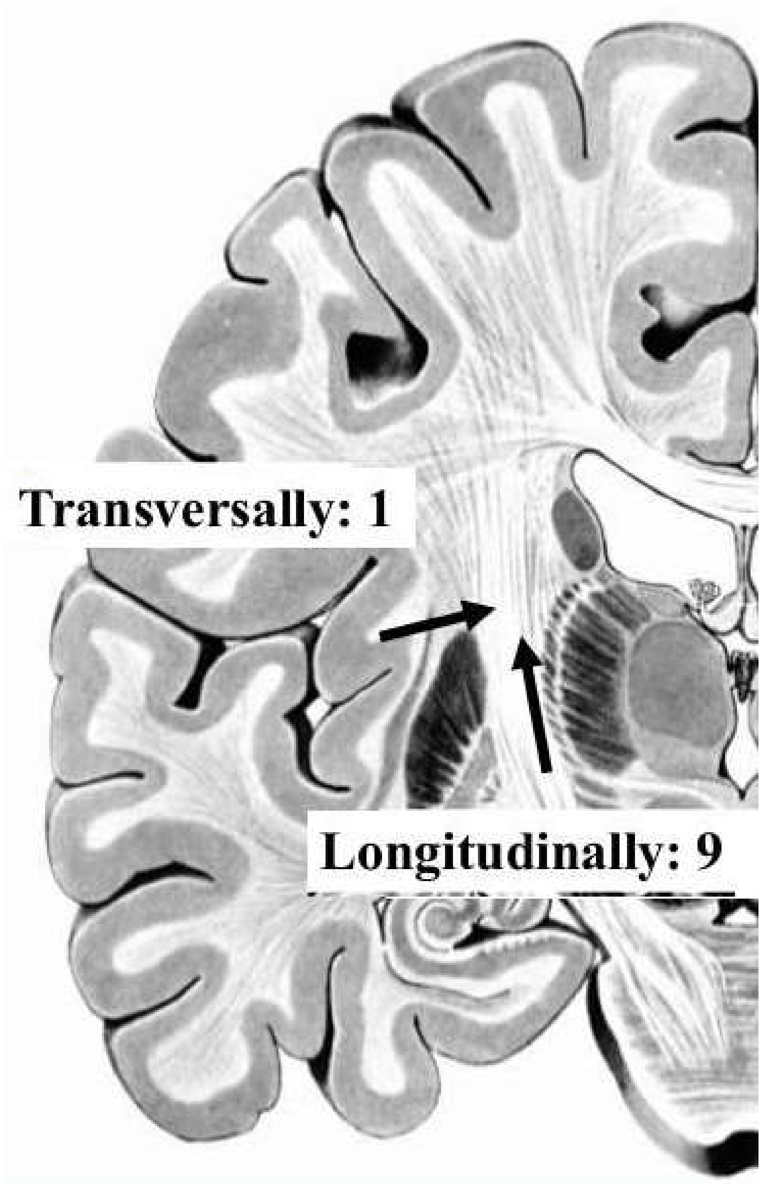

anisotropy of White Matter

isotropic case: $\boldsymbol{\sigma} = \boldsymbol{\sigma}_0 I$, anisotropic: $\boldsymbol{\sigma} = UDU^{\mathsf{H}}$.

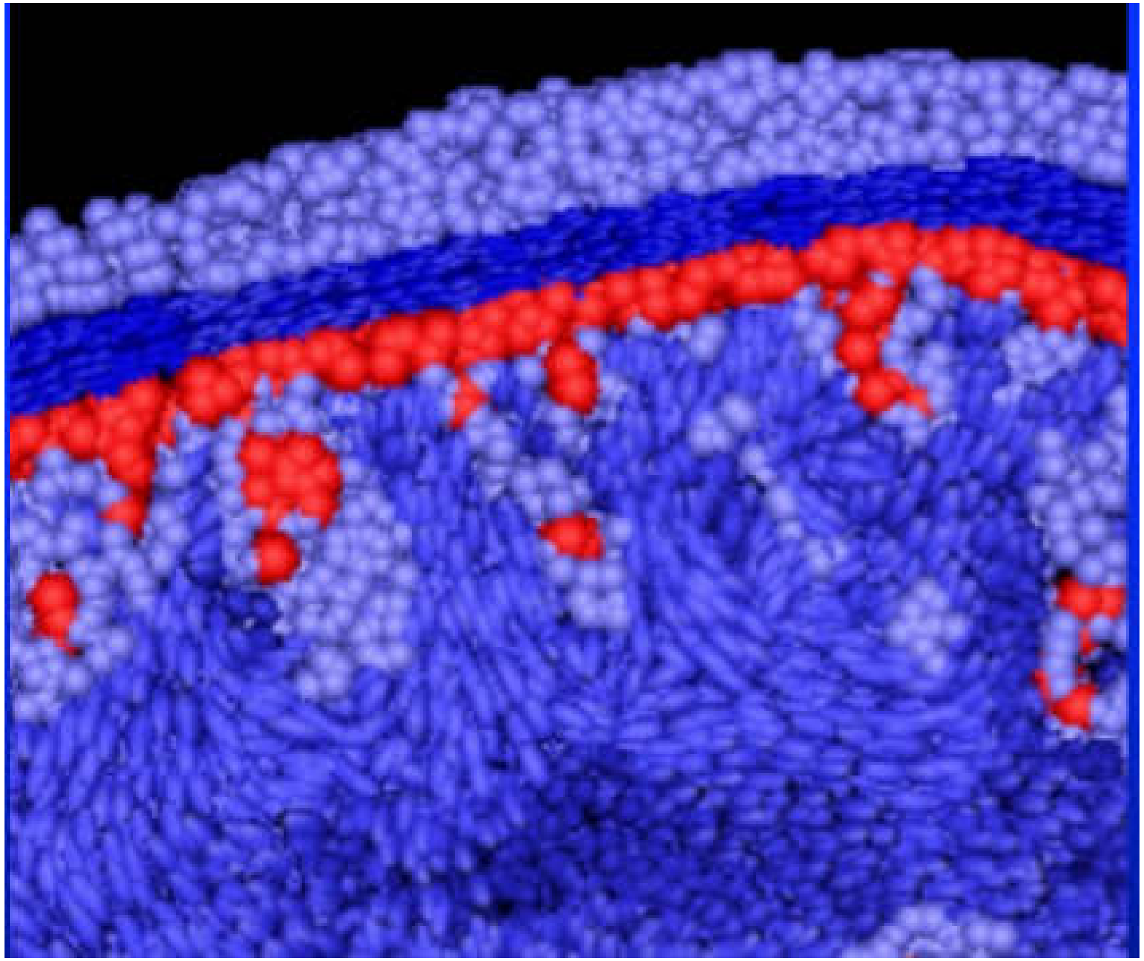

illustration of the anisotropic behaviour

Details:

1) Scalp: $\sigma = 0.33$ S/m

2) Skull: higher conductivity in tangential direction, smaller conductivity in normal(radial) direction: $\sigma_2^{\text{rad}} = 0.0042$ S/m, $\sigma_2^{\text{tang}} = 0.042$ S/m

♦ The mesh has to be located inside the skull compartment.

♦ The mesh has to approximate the outer surface of the skull spongiosa [Hueso esponjoso].

♦ The mesh has to be smooth, so that normal directions are not changing too strongly for neighboured points in the skull.

See §3.3 in

Carsten H. Wolters: Influence of Tissue Conductivity Inhomogeneity and Anisotropy on EEG/MEG base Source Localization in the Human Brain. Doctoral Thesis. Leipzig University, 2003

3) CSF (liquor): $\sigma = 1.79$ S/m

4) White matter: See §3.4

5) Gray matter: $\sigma = 0.33$ S/m

3.2 Finite Element Accuracy

Scenario 1:

Piecewise linear finite elements of size h, smooth coefficients of L smooth, smooth boundary of Ω (or convex).

Then $f \in L^2(\Omega)$ implies that the solution of $Lu = f$ satisfies $u \in H^2(\Omega)$.

FE space $V_h \subset H^1(\Omega)$. FE triangulation: T_h. FE solution $u_h \in V_h$.

Lemma of Céa:

$$\|u - u_h\|_{H^1(\Omega)} \leq C \inf_{w \in V_h} \|u - w\|_{H^1(\Omega)} = C \left[\inf_{w \in V_h} \sum_{\Delta \in T_h} \|u - w\|^2_{H^1(\Delta)} \right]^{1/2}$$

leads to

$$\|u - u_h\|_{H^1(\Omega)} \leq C' h \, \|u\|_{H^2(\Omega)} \leq C'' h \, \|f\|_{L^2(\Omega)} .$$

With the help of the adjoint problem we get $\|u - u_h\|_{L^2(\Omega)} \leq ch \, \|u - u_h\|_{H^1(\Omega)}$, so that

$$\|u - u_h\|_{L^2(\Omega)} \leq Ch^2 \, \|f\|_{L^2(\Omega)} .$$

Scenario 2:

As in Scenario 1, but the coefficients of L are only piecewise smooth, e.g. smooth (or even constant) in $\Omega_1 \subset \Omega$ and $\Omega_2 \subset \Omega$ with the interior boundary $\gamma := \partial\Omega_1 \cap \partial\Omega_2$.

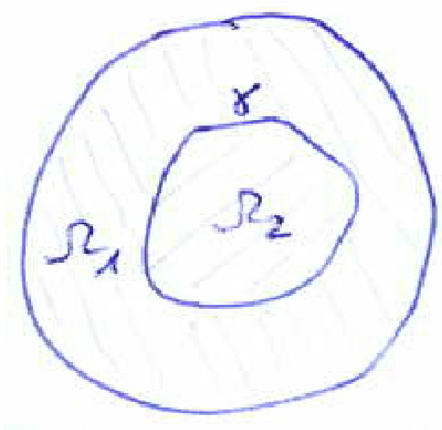

Then $f \in L^2(\Omega)$ does not imply $u \in H^2(\Omega)$, but $u|_{\Omega_1} \in H^2(\Omega_1)$ and $u|_{\Omega_2} \in H^2(\Omega_2)$.

If the finite elements are aligned with the interior boundary γ, each finite element $\Delta \in T_h$ satisfies either $\Delta \subset \Omega_1$ or $\Delta \subset \Omega_2$. Hence each term $\|u - w\|^2_{H^1(\Delta)}$ in $\|u - u_h\|_{H^1(\Omega)} \leq C \left[\inf \left\{ \sum_{\Delta \in T_h} \|u - w\|^2_{H^1(\Delta)} \right\} : w \in V_h \right]$ yields the same estimate as before. Hence

$$\|u - u_h\|_{L^2(\Omega)} \leq Ch^2 \, \|f\|_{L^2(\Omega)} \,.$$

Scenario 3: The divergence of the **Delta function** does not satisfy $f \in L^2 \Longrightarrow$ loss of accuracy

4 Subtraction Approach

General form of the Subtraction Approach:

Assume that we want to solve a linear PDE

$$Lu = f \qquad \text{with} \quad f = g + d_0.$$

Solution of $Lu_1 = g$ possible, but solution of $Lu_2 = d_0$ difficult (e.g. since d_0 has a singularity).

Assumption: u_0 is the solution of

$$L_0 u_0 = d_0$$

with another differential operator $L_0 \neq L$.

We try to represent the solution of $Lu = f$ by the ansatz

$$u = u_0 + u^{\text{corr}}.$$

Repeated: $Lu = f = g + d_0,\ L_0 u_0 = d_0,\ u = u_0 + u^{\text{corr}}$.

Then u^{corr} is the solution of

$$\begin{aligned} Lu^{\text{corr}} &= L(u - u_0) \\ &= Lu - Lu_0 \\ &= g + d_0 - Lu_0 \\ &= g + L_0 u_0 - Lu_0 \\ &= g + (L_0 - L)\, u_0. \end{aligned}$$

Possibly, the right-hand side $g + (L_0 - L)\, u_0$ is more regular and

$$Lu^{\text{corr}} = g + (L_0 - L)\, u_0$$

is easier to solve.

We recall: $Lu = \text{div}\,(\boldsymbol{\sigma}\,\text{grad}\,u) = J := \text{div}\,\mathbf{j}$ with $\mathbf{j}(\mathbf{x}) := \mathbf{M}\delta(\mathbf{x}-\mathbf{x}_0)$.

Assumption: $\mathbf{x}_0 \in \Omega_0$, where Ω_0 is an (open) domain with constant $\boldsymbol{\sigma} = \boldsymbol{\sigma}_0 I$.

Then

$$u_0(\mathbf{x}) := \frac{1}{4\pi\boldsymbol{\sigma}_0}\frac{\langle \mathbf{M}, \mathbf{x}-\mathbf{x}_0\rangle}{|\mathbf{x}-\mathbf{x}_0|}$$

is the solution of

$$L_0 u_0 = \text{div}\,(\boldsymbol{\sigma}_0\,\text{grad}\,u_0) = \mathbf{j} = \text{div}\,\mathbf{M}\delta(\cdot-\mathbf{x}_0) \quad \text{in } \mathbb{R}^3.$$

Proof: $L_0 = \boldsymbol{\sigma}_0\Delta$, use the well known Green function of the Laplace equation.

REMARK: $u_0(\mathbf{x})$ is bounded, but discontinuous at $\mathbf{x} = \mathbf{x}_0$.
On the other hand, $u_0(\mathbf{x})$ is analytic in $\mathbb{R}^3 \backslash \{\mathbf{x}_0\}$.
The larger $|\mathbf{x}-\mathbf{x}_0|$, the smoother is u_0.

The desired solution u is the sum $u_0 + u^{\text{corr}}$ with u^{corr} being the solution of

$$\operatorname{div}(\boldsymbol{\sigma} \operatorname{grad} u^{\text{corr}}) = \begin{cases} -\operatorname{div}((\boldsymbol{\sigma} - \boldsymbol{\sigma}_0) \operatorname{grad} u_0) & \text{in } \Omega \backslash \Omega_0 \\ 0 & \text{in } \Omega_0 \end{cases}$$

$$\left\langle \boldsymbol{\sigma}, \frac{\partial u^{\text{corr}}}{\partial \mathbf{n}} \right\rangle = -\left\langle \boldsymbol{\sigma}, \frac{\partial u_0}{\partial \mathbf{n}} \right\rangle \qquad \text{on } \Gamma.$$

Now, u^{corr} is smooth enough:

support of r.h.s. in $\Omega \backslash \Omega_0$ and $|\mathbf{x} - \mathbf{x}_0| \geq \operatorname{dist}(\mathbf{x}_0, \partial\Omega_0) > 0$ for $\mathbf{x} \in \Omega \backslash \Omega_0$

$\Rightarrow -\operatorname{div}((\boldsymbol{\sigma} - \boldsymbol{\sigma}_0) \operatorname{grad} u_0) \in L^2(\Omega)$ (even $\ldots \in L^\infty(\Omega)$).

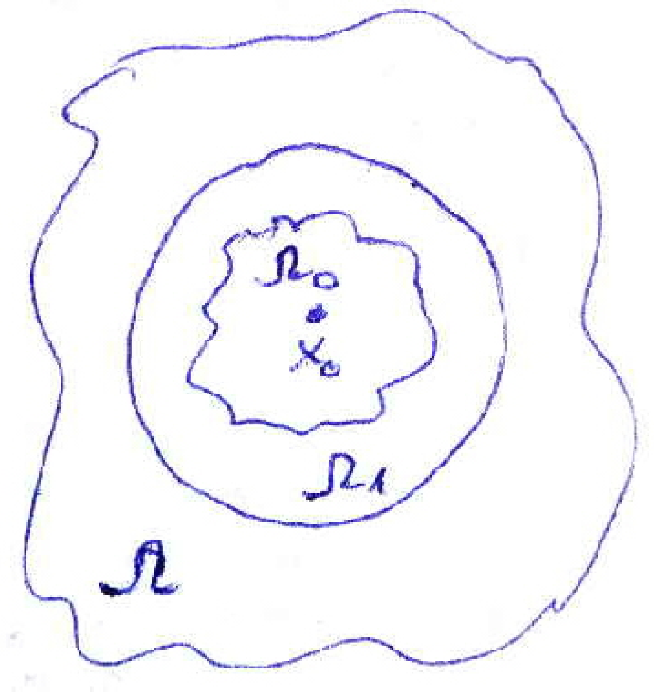

Modification: Replace u_0 by χu_0 with a cut-off function χ,

i.e., $\chi = 1$ in a neighbourhood Ω_0 of $\mathbf{x}_0$,

χ smooth, $\chi = 0$ outside of Ω_1: $\Omega_0 \subset\subset \Omega_1 \subset\subset \Omega$.

Literature:

C.H. Wolters, L. Grasedyck, W. Hackbusch: *Efficient computation of lead field bases and influence matrix for the FEM-based EEG and MEG inverse problem*. Inverse Problems **20** (2004) 1099-1116

C. Wolters, H. Köstler, C. Möller, J. Härdtlein, L. Grasedyck, W. Hackbusch: *Numerical mathematics for the modeling of a current dipole in EEG source reconstruction using finite element head models.* SIAM J. on Scientific Computing **30**:24-45, 2007.

F. Drechsler, C. Wolters, T. Dierkes, H. Si, L. Grasedyck: *A highly accurate full subtraction approach for dipole modelling in EEG source analysis using the finite element method.* NeuroImage **46**:1055-1065, 2009.

M. Höltershinken, P. Lange, F. Wallois, A. Buyx, S. Pursiainen, C. Engwer, C. Wolters: *The Localized Subtraction Approach For EEG and MEG Forward Modeling.* Proceedings of the workshop BIOSIGNAL 2022, Aug. 24- 26, 2022, Dresden, Germany

T. Erdbrügger, A. Westhoff, M. Höltershinken, J. Radecke, Y. Buschermöhle, A. Buyx, F. Wallois, S. Pursiainen, J. Gross, R. Lencer, C. Engwer, C. Wolters: *CutFEM forward modeling for EEG source analysis.* 2022. `https://arxiv.org/abs/2211.17093`

E. Bejaoui, F. Ben Belgacem: *Singularity extraction for elliptic equations with coefficients with jumps and Dirac sources*. Asymptotic Analysis, 2023 - DOI: 10.3233/ASY-221824

5 Lead Field Matrix

5.1 Definition

Let

$$K_h u_h = f_h$$

be the FE equation. h characterised the FEM, K_h is the stiffness matrix, u_h the coefficient vector of the FE solution for the right-hand side f_h.
In our application, we have very many right-hand sides $f_h = d_j$ corresponding to dipoles at x_j ($j \in J$).
The i-th sensor detects the value $R_i u_h \in \mathbb{R}$ (R_i: restriction, $i \in I$).

$R_i u_h = R_i K_h^{-1} d_j$ gives rise to the so-called Lead Field Matrix

$$\mathbf{L} = \left(R_i K_h^{-1} d_j\right)_{(i,j)\in I\times J} = \boxed{}\,.$$

$\mathbf{L}_{ij}$ describes the value of the i-th sensor caused by a dipole at x_j.

Index sets: $i \in I$, $j \in J$. Here, I is of moderate size†, whereas J is very large (all possible positions of the dipole).

†Up to 512 electrods for EEG,
see https://www.compumedics.com.au/en/products/neuvo-64-512-channel-eeg-hd-ltm-eeg/

5.2 Efficient Computation

Solving $K_h u_h^{(j)} = d_j$ for all $j \in J$ requires $\#J$ solves $\Rightarrow$ too costly

Remedy: The restriction $R_i u_h \in \mathbb{R}$ is a linear functional and can be described by a scalar product $\langle r_i, u_h \rangle \Rightarrow$

$$R_i u_h^{(j)} = \left\langle r_i, u_h^{(j)} \right\rangle = \left\langle r_i, K_h^{-1} d_j \right\rangle = \left\langle K_h^{-\mathsf{T}} r_i, d_j \right\rangle .$$

Therefore, solve the adjoint problem $K_h^{\mathsf{T}} v_i = r_i$ for all $i \in I$. Then

$$\mathbf{L}_{ij} = R_i u_h^{(j)} = \left\langle v_i, d_j \right\rangle$$

requires only $\#I << \#J$ solves.

5.3 Inverse Problem

In general, the inverse problem is ill-posed (there are right-hand sides (sources) $f_h \neq 0$ so that the corresponding solution u_h of $K_h u_h = f_h$ leads to $R_i u_h = 0$).

A-priori information must be added:

- source location: dipole $\mathbf{M}_j \delta(\mathbf{x} - \mathbf{x}_j)$ at a single spot $\mathbf{x}_j$ $(j \in J)$

- only $\mathbf{x}_j$ located on the folded surface of the brain inside the cortex (cortex contained in the grey matter)

- direction of $\mathbf{M}_j$ perpendicular to the surface.

The source model

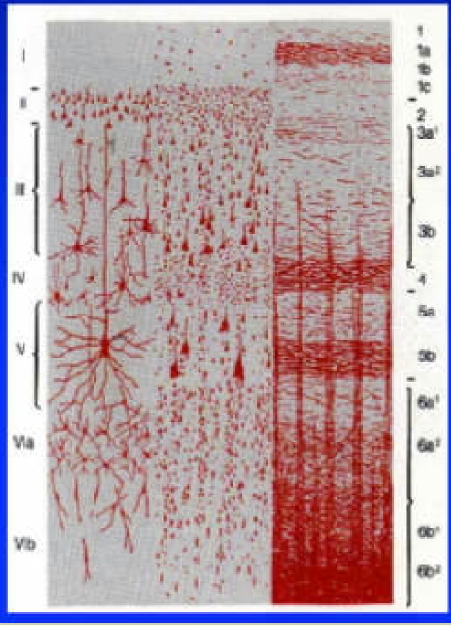

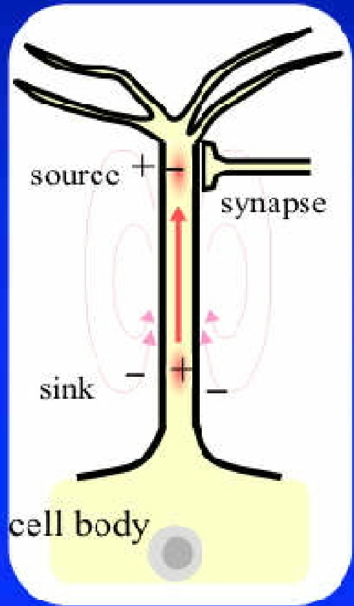

Microscopic current flow (~5×10^{-5} n

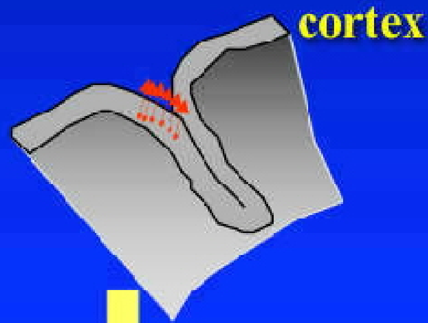

Equivalent Current Dipole (Primary current) (~50 nAm)

parameters:

position : x_0

moment : M

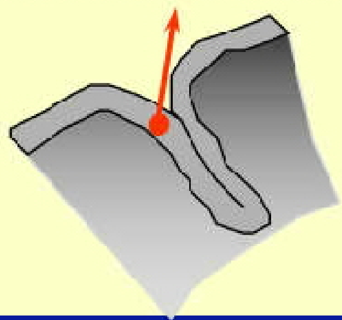

Size of Macroscopic Neural Activity

~30 mm^2 = **5.5×5.5 mm^2**

$\Rightarrow$

$$\|\mathbf{L}w - \mathbf{m}\| = \min_{w}, \ w \text{ subject of } \|w\|_0 = 1,$$

with

$\mathbf{L}$: lead field matrix,

$\mathbf{m}$: vector of measurements.

$\|w\|_0 = 1$ corresponds to the sparse optimisation!

E.g., solution as follows: $\hat{m} = \mathbf{m} / \|\mathbf{m}\|_2$,

ℓ_j : j-th column of $\mathbf{L}$. Set $\hat{\ell}_j := \ell_j / \left\|\ell_j\right\|_2$, $\hat{\ell}_j = \ell_j^{||} + \ell_j^{\perp}$ with $\ell_j^{||} = \left\langle \hat{\ell}_j, \hat{m} \right\rangle \hat{m}$.

Optimal w is e_{j^*} with $j^* = \arg\min_j \{ \left\|\ell_j^{\perp}\right\|_2 \}$.

6 Literature

Concerning the **inverse problem**:

Chapter 6 of
Carsten H. Wolters: *Influence of Tissue Conductivity Inhomogeneity and Anisotropy on EEG/MEG base Source Localization in the Human Brain.* Doctoral Thesis. Leipzig University, 2003

F. Lucka, S. Pursiainen, M. Burger, C.H. Wolters: *Hierarchical Bayesian Inference for the EEG Inverse Problem using Realistic FE Head Models: Depth Localization and Source Separation for Focal Primary Currents.* NeuroImage, 61(4), pp.1364–1382, (2012).

These and many more publications can be obtained from
`https://www.medizin.uni-muenster.de/fileadmin/einrichtung/biomag/Mitarbeiter/Wolters-Publications.pdf`

7 Software

DUNEuro: A free and open-source C++ software toolbox for the numerical computation of forward solutions in bioelectromagnetism:

`https://journals.plos.org/plosone/article?id=10.1371/journal.pone.0252431`

`https://www.medizin.uni-muenster.de/duneuro/startseite.html`

8 Next Parts

Size of the FE matrix K_h: up to several millions.

Next Topics:

- **Multigrid Iteration**
- **Technique of Hierarchical Matrices**